

Revisiting Einstein's analogy: black holes as gradient-index lenses

J. E. Gómez-Correa,^{1,*} E. Espíndola-Ramos,^{1,†} O. López-Cruz,^{1,‡} and S. Chávez-Cerda^{1,§}

¹*Instituto Nacional de Astrofísica, Óptica y Electrónica,
Santa María Tonantzintla, Puebla, 72840, Mexico*

Abstract

According to Albert Einstein, gravitation is analogous to an optical medium. Building on this idea, various definitions of the gradient-index (GRIN) medium representing curved spacetime have been proposed; often, these approaches demand advanced knowledge of General Relativity and its associated mathematical methods. This paper introduces a novel approach for generating the form of GRIN media that reproduces the behavior of light in the presence of a Schwarzschild black hole or about the equatorial spacetime of a Kerr black hole. Our approach is based on Noether's theorem that leads to optical Fermat's principle, leveraging the system's symmetry, resulting in a general method for finding GRIN media in a flat spacetime that reproduces the behavior of light in Schwarzschild-like spacetimes where *only using photon trajectories as input*. This approach is also valid for material particles and provides a complementary understanding of General Relativity.

* jgomez@inaoep.mx

† ernestoespindola@inaoep.mx

‡ omarlx@inaoep.mx

§ sabino@inaoep.mx

I. INTRODUCTION

Gravitational lensing is the phenomenon where the trajectory of waves or particles is deflected due to the curvature of spacetime. Predicted by Einstein's theory of General Relativity, this phenomenon has been explored through various spacetime solutions to Einstein's field equations, demonstrating to be a powerful tool for studying the universe [1, 2].

Many astrophysical studies rely on strong, weak, and microlensing phenomena to understand galaxy clusters' structure and mass distribution. As natural cosmic lenses, these phenomena have led to the discovery of exoplanets beyond our solar system and have the potential to extend our observational capabilities beyond light. With advancements in gravitational wave detectors, the possibility of detecting lensed gravitational waves is increasing. For a comprehensive review of these subjects, refer to [1–4].

The deflection of light is often described using the thin-lens approximation. However, the direct detection of gravitational waves by the Laser Interferometer Gravitational-Wave Observatory (LIGO) [5] and the observation of the black hole at the center of our galaxy by the Event Horizon Telescope collaboration (EHT) [6] promote the use of the complete theory of General Relativity. Although phenomena involving the strong effects of curved spacetime are beyond our capacity to directly experience or experiment with, analogies with other branches of physics, such as classical mechanics, quantum mechanics, optics, and fluid mechanics [2, 7–15], may enable their study in the laboratory.

Approaches to studying light propagation in curved spacetimes using concepts from optics and variational principles have been explored since the birth of general relativity. As noted in Ref. 8, "*the idea that gravitation is equivalent to an optical medium was first suggested by Einstein himself.*" Key concepts along this path include Maxwell's equations in general relativity as electrodynamics in a macroscopic medium [7, 8], the optical metric [16], and a relativistic version of Fermat's principle [17], among others.

Metamaterials allow the reproduction of electromagnetic waves in curved spacetimes through the formal equivalence between Maxwell's equations in general relativity and those of electrodynamics in a macroscopic medium. However, reproducing light rays through GRIN media is advantageous when polarization effects are disregarded, as it is much simpler and easier to construct experimentally [14]. Currently, various definitions of the gradient index for curved spacetime exist; therefore, as pointed out in Ref. 18, the best way to find

the most precise definition is by comparing the null geodesics in spacetime with light rays in the optical media.

Noether’s theorem, one of the most fascinating theorems in modern physics, was inspired by Albert Einstein’s work on relativity. It states that a natural law described by a Lagrangian function that exhibits symmetry has an invariant, also called conserved quantity. The associated Euler–Lagrange equations inherit the symmetry group of the variational problem [19]. In general, variational principles are related to finding extrema, that in physical systems are commonly minima. In this sense, Fermat’s principle states that a ray of light traveling in a medium with variable refractive index will take the route that minimizes the time of travel between two given points, which can be expressed as a variational principle yielding to the corresponding Euler-Lagrange equations, simplifying substantially the problem.

Suppose the Geometrical Optics formalism is used alone. In that case, finding the path of a ray of light in Gradient-Index (GRIN) media is cumbersome since it requires finding the solution of a partial differential equation called the Eikonal. Different methods have been proposed to solve this equation, but their implementation is complicated and is restricted to a medium with a specific GRIN distribution.

In recent decades, the inverse problem—finding the GRIN distribution for a given light ray path—has garnered increasing attention. Since this task may be even more challenging than determining ray propagation in a GRIN medium, the methods proposed in the literature have different complexity. However, it has been demonstrated that an exact method for solving the inverse problem in any symmetric GRIN medium can be derived using Noether’s invariant of the system [20]. This approach, known as the Physical GRIN Reconstruction (PhysGRIN) method, enables the determination of the refractive index at any point within the medium based on the ray direction and Noether’s invariant. Following the ray’s path and employing the invariant effectively defines the symmetric refractive index distribution. Once the ray trajectories are established, the algorithm is easily implemented and computationally efficient. This method can be extended to other areas of physics being formulated using variational principles, such as astronomy [21–25].

In this paper, using the PhysGRIN method and leveraging the trajectory of a photon around the equatorial Kerr black hole, we introduce a novel approach for constructing GRIN lenses that replicate photon paths in the curved spacetime of these black holes. Inspired by Einstein’s analogy between gravitation and optical media, this method allows us to create

GRIN models of curved spacetime without requiring advanced knowledge of general relativity or tensor calculus, instead relying on Noether's theorem and the system's symmetry.

II. PHOTON TRAJECTORIES AROUND EQUATORIAL KERR BLACK HOLES

The Schwarzschild metric is one of the most studied models of black holes; it is the unique, static, spherically symmetric vacuum solution to Einstein's field equations and forms the basis for the theory of gravitational lensing [21]. It is also a particular case of the Kerr spacetime, which generalizes it to include the effects of rotation.

The infinitesimal interval of events for a Kerr black hole of mass M in Boyer–Lindquist coordinates is given by

$$ds^2 = -c^2 \left(1 - \frac{2GM r_{bl}}{c^2 \Sigma} \right) dt^2 - \frac{4GM r_{bl} a \sin^2 \theta}{c^2 \Sigma} c dt d\phi + \left(r_{bl}^2 + a^2 + \frac{2GM r_{bl} a^2}{c^2 \Sigma} \sin^2 \theta \right) \sin^2 \theta d\phi^2 + \frac{\Sigma}{\Delta} dr_{bl}^2 + \Sigma d\theta^2, \quad (1)$$

where G denotes the universal gravitational constant, c the speed of light, a is related to the angular momentum J of the black hole by $a = J/Mc$, (r_{bl}, θ, ϕ) are related to the Cartesian coordinates by $x_c = \sqrt{r_{bl}^2 + a^2} \sin \theta \cos \phi$, $y_c = \sqrt{r_{bl}^2 + a^2} \sin \theta \sin \phi$, and $z_c = r_{bl} \cos \theta$, and

$$\Sigma = r_{bl}^2 + a^2 \cos^2 \theta, \quad \Delta = r_{bl}^2 - \frac{2GM r_{bl}}{c^2} + a^2. \quad (2)$$

This metric has two coordinate singularities determined by $\Delta = 0$. The exterior singularity, $r_{bl,+} = [GM + \sqrt{G^2 M^2 - c^4 a^2}] / c^2$, is known as the outer event horizon and marks the boundary beyond where nothing can escape. The interior singularity, $r_{bl,-} = [GM - \sqrt{G^2 M^2 - c^4 a^2}] / c^2$, is called the inner event horizon or Cauchy horizon, and marks the region where spacetime becomes unstable [26]. These coordinate singularities restrict the black hole's angular momentum, which must satisfy $-GM/c \leq a \leq GM/c$ for $r_{bl,+}$ and $r_{bl,-}$ to be real.

The Kerr metric also contains a true singularity at $r_{bl} = 0$ and $\theta = \pi/2$, where $\Sigma = 0$, causing the curvature to become infinite. This singularity forms a ring of radius a at the equator. Unlike the Schwarzschild metric ($a = 0$), the coefficient of dt^2 in the Kerr metric changes sign at a region different from the event horizon, known as the ergosphere. The boundary of the ergosphere is given by $r_{bl,e} = [GM + \sqrt{G^2 M^2 - a^2 c^4 \cos^2 \theta}] / c^2$, which is exterior to the event horizon except at the poles ($\theta = 0, \pi$), where they coincide. Inside the

ergosphere, static particles ($dr_{bl} = d\theta = d\phi = 0$) are not possible because their worldlines would be forced to move in the direction of the black hole's angular momentum due to the dragging effect of spacetime.

Eq. (1) can be summarized using the metric tensor notation as follows:

$$ds^2 = g_{\alpha\beta} dx^\alpha dx^\beta, \quad (3)$$

where the upper and lower indices denote Einstein's summation notation, with $\alpha, \beta = 0, 1, 2, 3$, and $x^0 = ct$, $x^1 = r$, $x^2 = \theta$, and $x^3 = \phi$. The world line of a particle, which represents the path that the particle traces in spacetime, is a one-dimensional curve in four-dimensional spacetime. This curve can be parametrized by a parameter λ , which labels every point along the trajectory. For massive particles, it is convenient to identify λ with the particle's proper time τ . However, proper time is useless for massless particles like photons, so λ is used instead. The parameterization of the world line is denoted as

$$\mathbf{x} = (x^0(\lambda), x^1(\lambda), x^2(\lambda), x^3(\lambda)). \quad (4)$$

The standard approach to null geodesics is through the Lagrangian formalism, though they can also be expressed in the Hamiltonian formalism. A brief discussion on these formalisms and the challenges of computing particle or photon trajectories can be found in Ref. 22. Since we are interested in geodesics confined to the equatorial plane to exploit spherical symmetry for GRIN medium reconstruction, the most straightforward approach is via Lagrangian formalism. The Lagrangian associated with the metric (3) is given by:

$$\mathcal{L} = \frac{1}{2} g_{\alpha\beta} \dot{x}^\alpha \dot{x}^\beta, \quad (5)$$

where $\dot{x}^\alpha = dx^\alpha/d\lambda$ denotes the components of the four-velocity. The term $g(\dot{x}, \dot{x}) \equiv g_{\alpha\beta} \dot{x}^\alpha \dot{x}^\beta$ represents the square of the norm of the four-velocity, which for photons equals zero, as the four-velocity vector lies on the local light cone. Under these conditions, null geodesics (world lines of photons) satisfy the following system of equations:

$$\mathcal{L} = 0, \quad \frac{d}{d\lambda} \frac{\partial \mathcal{L}}{\partial \dot{x}^\alpha} - \frac{\partial \mathcal{L}}{\partial x^\alpha} = 0. \quad (6)$$

A review and classification of trajectories using elliptic integrals of the first and third kind, Carlson's elliptic integrals, Jacobi-elliptic functions, and Weierstrass elliptic functions, along with codes for computing geodesics in Wolfram Mathematica and Fortran, can be found in Ref. 27–32.

For convenience, let us define $m_b \equiv GM/c^2$ and $T = ct$. The geodesics lying in the equatorial plane must satisfy $\theta = \pi/2$ and $\dot{\theta} = 0$. A direct insight is that the Kerr metric (and thus the Lagrangian) does not depend explicitly on t and ϕ . Therefore, we have the following two integrals [33]:

$$\begin{aligned} \left(1 - \frac{2m_b}{r_{bl}}\right) \dot{T} + \frac{2m_b a}{r_{bl}} \dot{\phi} &= \frac{E}{c} \equiv \varepsilon, \\ \left(r_{bl}^2 + a^2 + \frac{2m_b a^2}{r_{bl}}\right) \dot{\phi} - \frac{2m_b a}{r_{bl}} \dot{T} &\equiv L, \end{aligned} \quad (7)$$

where E and L are the energy per unit mass and the angular momentum per unit mass, respectively. Thus, \dot{T} and $\dot{\phi}$ can be determined in terms of r_{bl} , L , and ε , and substituted into $ds^2 = 0$ (the condition for null geodesics, equivalent to $\mathcal{L} = 0$), and an equation for \dot{r}_{bl} is derived [33].

$$r_{bl}^2 \dot{r}_{bl}^2 = (r_{bl}^2 + a^2) \varepsilon^2 - L^2 + \frac{2m_b}{r_{bl}} (a\varepsilon - L)^2. \quad (8)$$

Since we are only interested in the trajectories of photons, we can eliminate the dependence on the affine parameter as $\dot{\phi}/\dot{r}_{bl} = d\phi/dr_{bl}$, which can be rewritten as [29]

$$d\phi = \frac{hr_{bl}^2 - 2m_b r_{bl}(h - a)}{\Delta\sqrt{N}} dr_{bl}, \quad (9)$$

where

$$h = \frac{L}{\varepsilon}, \quad N = r_{bl}^4 + r_{bl}^2(a^2 - h^2) + 2m_b r_{bl}(a - h)^2. \quad (10)$$

When $h = a$, the integration of Eq. (9) is straightforward [33]

$$\phi = \frac{a}{r_{bl,-} - r_{bl,+}} \ln \left(\frac{r_{bl} - r_{bl,-}}{r_{bl} - r_{bl,+}} \right). \quad (11)$$

The resulting trajectories play the same role as the radial geodesics in the Schwarzschild geometry [33]. Fig. 1 shows radial geodesics for a Kerr black hole rotating clockwise for $a = 0.1m_b$, and $0.9m_b$. According to Ref. 29, Eq. (9) can be integrated exactly in terms of elliptic integrals of the first and third kinds [34] when integrating from the point $r_{bl,0}$, where the distance from the geodesic to the event horizon is minimized, to the position r_{bl} , with $r_{bl} > r_{bl,0}$. By reparametrizing $r_{bl} = 2m_b x$, $a = 2m_b j$, and $h = 2m_b \psi$, where x, j, ψ are dimensionless, this condition of minima distance is equivalent to [29]

$$f(x_0) = x_0^4 + (j^2 - \psi^2)x_0^2 + (j - \psi)^2 x_0 = 0. \quad (12)$$

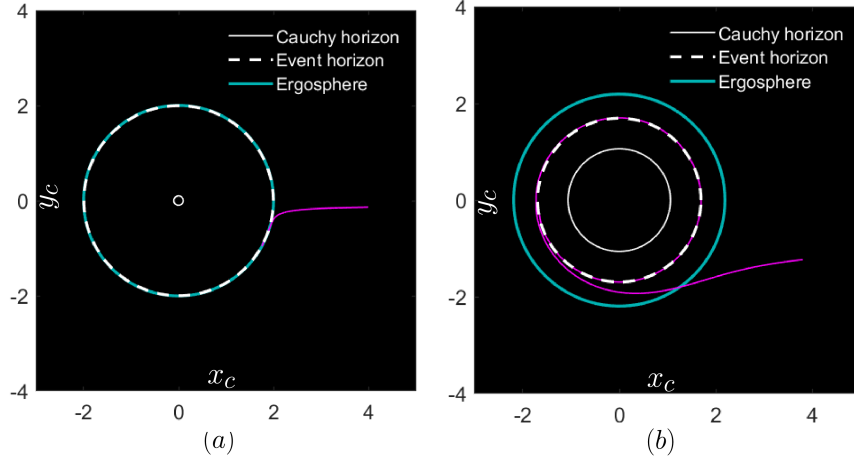


FIG. 1. Radial geodesics ($h = a$) are shown for the cases (a) $a = 0.1$ and (b) $a = 0.9$, using Planck units and $m_b = 1$. Cartesian coordinates x_c and y_c were used.

Thus, for a given value of x_0 , ψ is determined [29]:

$$\psi_{\pm} = \frac{-j \pm x_0 \sqrt{x_0^2 - x_0 + j^2}}{x_0 - 1}, \quad (13)$$

where \pm indicates prograde and retrograde trajectories. The explicit form of the exact solution to these null geodesics can be found in Ref. 29. However, it is important to note a misprint in Eq. (17) in that article: the variable z should be replaced with $\sin(z)$. Under these conditions, it is straightforward to demonstrate that when $j = 0$, the results in Ref. 29 reduce to the Schwarzschild case, as shown in Ref. 35. Fig. 2 presents the analytical prograde and retrograde geodesics for the cases (a) $a = 0.1m_b$ and (b) $a = 0.9m_b$ with $r_{bl,0} = 4m_b$.

As a first attempt to extend our analysis, Eq. (9) is integrated numerically using the trapezoidal method, selecting values of ψ within the range (ψ_-, ψ_+) that ensure the coefficient in Eq. (9) remains real-valued throughout the interval (x_0, x) . Fig. 2 shows the numerically computed paths for the cases (a) $a = 0.1m_b$ and (b) $a = 0.9m_b$, with $r_{bl,0} = 4m_b$. It follows that these numerical paths escape from the black hole.

As we are interested in reproducing light trajectories around a black hole using a symmetric GRIN media, we mainly focus on trajectories that cross the event horizon. To obtain such trajectories through numerical integration, we first need to ensure that the coefficient of dr in Eq. (9) is a real-valued function, which implies that the values of ψ must be restricted. This restriction arises from the condition $f(x) > 0$ for the interval $x \in (0, \infty)$, which can be

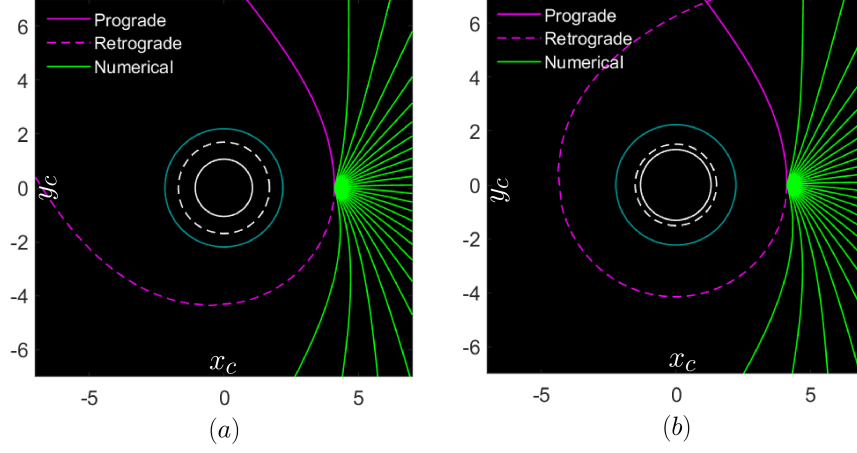


FIG. 2. Exact prograde and retrograde paths and numerical null geodesics for the cases (a) $a = 0.9$ and (b) 0.99 , using Planck units and $m_b = 1$, and the point of convergence at $r_{bl,0} = 4$. Cartesian coordinates x_c and y_c were used.

reduced to

$$g(x) \equiv x^3 + (j^2 - \psi^2)x + (j - \psi)^2 > 0. \quad (14)$$

Since $g(x)$ is a cubic function of x with a positive coefficient for x^3 , the inequality Eq. (14) is satisfied if the evaluation of $g(x)$ at the critical value

$$x_{critical} = \frac{\sqrt{\psi^2 - j^2}}{\sqrt{3}}, \quad (15)$$

is positive. The roots of $g(x_{critical}) = 0$ lead to the condition

$$(j - \psi)^2 = \frac{2(\psi^2 - j^2)^{3/2}}{3\sqrt{3}}. \quad (16)$$

Thus, by solving for ψ , it is found the range of values that ensures the numerical integration of Eq. (9) is well-defined:

$$\psi \in (\psi_1(j), \psi_2(j)), \quad (17)$$

where

$$\psi_1(j) = -j - \frac{3(1 + i\sqrt{3})}{4B(j)} - \frac{3}{4} (1 - i\sqrt{3}) B(j), \quad (18)$$

$$\psi_2(j) = \frac{1}{2} \left(-2j + \frac{3}{B(j)} + 3B(j) \right), \quad (19)$$

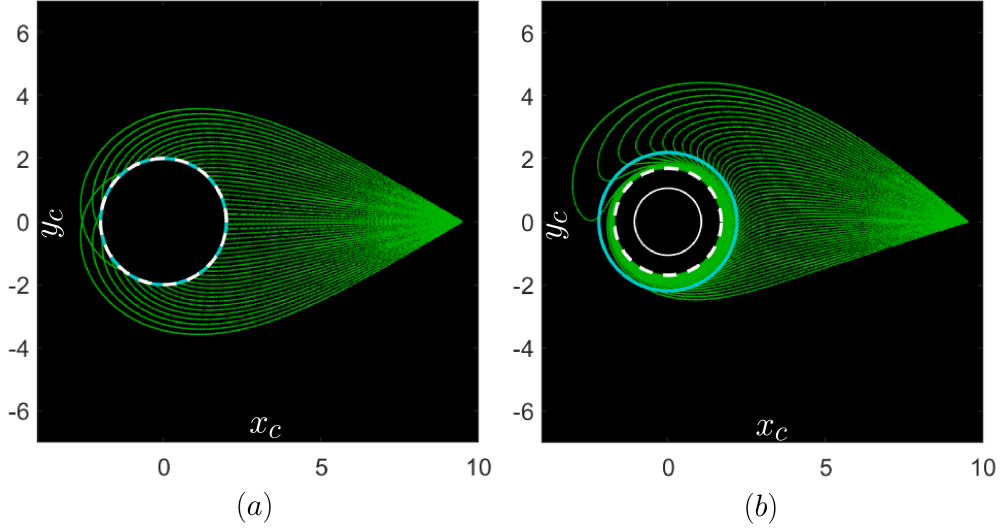


FIG. 3. Numerical null geodesics for the cases (a) $a = 0$ and (b) 0.9 , using Planck units and $m_b = 1$, and the position of convergence at $r_{bl,f} = 9.5$. Cartesian coordinates x_c and y_c were used.

and $B(j) = (-2j + \sqrt{4j^2 - 1})^{1/3}$. Finally, to ensure that all geodesics converge at the point $r_{bl,f}$ for all possible values of ψ , we integrate as follows:

$$\phi(x) = \int_{x_0}^x \frac{x'(\psi x' + j - \psi)}{(x'^2 + j^2 - x')\sqrt{f(x')}} dx' - \phi_0, \quad (20)$$

where

$$\phi_0 = \int_{x_0}^{x_f} \frac{x'(\psi x' + j - \psi)}{(x'^2 + j^2 - x')\sqrt{f(x')}} dx'. \quad (21)$$

Here, x_0 is chosen to be arbitrarily close to the exterior event horizon. In Fig. 3, it is shown the numerically computed paths using the trapezoidal method for $a = 0m_b$ and $0.9m_b$ by taking different values of ψ in the range Eq. (17); all trajectories converge at $r_{bl,f} = 9.5m_b$.

III. FERMAT'S RAY INVARIANT FOR GRIN MEDIA WITH SPHERICAL SYMMETRY

Fermat's principle can be expressed using orthogonal generalized coordinates associated with an arbitrary curvilinear orthogonal coordinate system that depends on a parameter τ ($q_1(\tau), q_2(\tau), q_3(\tau)$) as follows:

$$\delta \int_C \mathcal{L}(q_1, q_2, q_3; \dot{q}_1, \dot{q}_2, \dot{q}_3, \tau) d\tau = 0,$$

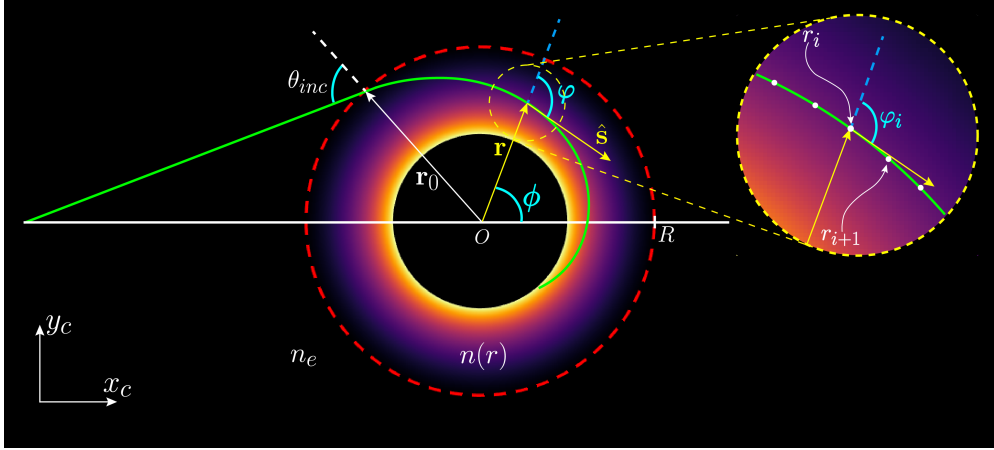


FIG. 4. The ray path propagating in a medium with a radially symmetric GRIN.

where, $\mathcal{L}(q_1, q_2, q_3; \dot{q}_1, \dot{q}_2, \dot{q}_3, \tau)$ is the optical Lagrangian, $\dot{q}_i = dq_i/d\tau$, with $i = 1, 2, 3$, and C represents the light-ray trajectories parameterized by τ . When using a spherical coordinate system (r, θ, ϕ) and a radially symmetric GRIN medium, it is sufficient to analyze the behavior of light along the equator ($\theta = \pi/2$), since any trajectories lie in a plane passing through the origin. This is the primary reason why the equatorial null geodesics of a Kerr black hole will be modeled using a spherical GRIN medium. Under these conditions, and by using r as the parameter of the trajectories, the Lagrangian function is given by:

$$\mathcal{L}(r) = n(r)\sqrt{1 + r^2\phi_r^2}, \quad (22)$$

with $\phi_r = d\phi/dr$. Thus, the light-ray trajectories satisfy the Euler-Lagrange equations [36], and since the Lagrangian does not explicitly depend on ϕ , there is a conserved quantity given by [20, 37]:

$$K = rn(r) \sin \varphi, \quad (23)$$

where φ is the angle between the vector $\hat{\mathbf{s}}$, tangent to the ray, and \mathbf{r} , as illustrated in Fig. 4. In optics, Eq. (23) is referred to as Fermat's ray invariant for inhomogeneous media with spherical symmetry [37, 38] or as Bouguer's formula [39].

It is important to emphasize that the value of K , once defined, does not change as the ray of light propagates. In other words, K is a conserved quantity along the light ray.

Equation (23) shows that Fermat's ray invariant depends on variations in the GRIN distribution. Therefore, the GRIN distribution can be determined if the value of K is known and the trajectory is given (thus, φ can be determined), as follows:

$$n(r) = \frac{K}{r \sin \varphi}, \quad (24)$$

The expression above forms the core of the PhysGRIN method for spherical symmetry. The numerical implementation to determine the refractive index for photon trajectories around a Kerr black hole will be analyzed in Sec. V.

IV. ANALYTICAL GRIN RECONSTRUCTION FROM PHOTON TRAJECTORIES

To determine the value of K , it is essential to know $\sin \varphi$. Consequently, as φ is the angle between $\hat{\mathbf{s}}$ and \mathbf{r} , the following relationship holds:

$$\sin \varphi = \frac{r(\phi)}{\sqrt{r^2(\phi) + \left(\frac{dr}{d\phi}\right)^2}}. \quad (25)$$

By substituting Eq. (25) into Eq. (24), the variation of the refractive index is given by:

$$n(r) = \frac{K \sqrt{r^2 + (dr/d\phi)^2}}{r^2}. \quad (26)$$

Now, let us assume that $n_e = n(R)$ and that $dr/d\phi$ can be expressed as a function of r , that is, $dr/d\phi = q(r)$. From Eq. (26), at $r = R$, we can derive K :

$$K = \frac{R^2 n_e}{\sqrt{R^2 + q^2(R)}}. \quad (27)$$

Then, Eq. (26) can be rewritten as:

$$n(r) = n_e \frac{R^2}{r^2} \sqrt{\frac{r^2 + q^2(r)}{R^2 + q^2(R)}}. \quad (28)$$

If we now consider the Boyer-Lindquist coordinates, it follows that:

$$q(r) = \frac{r_{bl}}{\sqrt{r_{bl}^2 + a^2}} \frac{dr_{bl}}{d\phi}. \quad (29)$$

Using Eq. (9), we find that for the most general case, the index of refraction is given by:

$$n(r) = n_e \frac{R^3}{r^3} \left| \frac{e(R)}{e(r)} \right| \sqrt{\frac{r^4 e^2(r) + s(r)}{R^4 e^2(R) + s(R)}}, \quad (30)$$

where

$$s(r) = \left[r^2 - 2m_b \sqrt{r^2 - a^2} \right]^2 \times \left[(r^2 - a^2)(r^2 - h^2) + 2m_b \sqrt{r^2 - a^2} (a - h)^2 \right], \quad (31)$$

and

$$e(r) = h \sqrt{r^2 - a^2} - 2m_b (h - a). \quad (32)$$

Equation (30) establishes the analytical distribution of the refractive index when the trajectories are represented in Cartesian coordinates x_c, y_c . Thus, Eq. (30) agrees with the observation made in Ref. 18 that the most accurate definition of the refractive index is achieved when light rays in optical media coincide with null geodesics.

Our model considers only GRIN media reproducing null geodesic trajectories; it does not include other electromagnetic effects, such as polarization.

Although the same approach to obtain the analytical form of the index of refraction was reported in Ref. 14, our results differ from theirs because they represented the null geodesics in Boyer-Lindquist coordinates (that is to say, the GRIN medium depends on the coordinate system used to visualize the trajectories); Additionally, they do not provide an explicit form of the proportionality constant K .

We use Cartesian coordinates instead of Boyer-Lindquist coordinates because, in such a representation, the singularity of the Kerr black hole appears as an annulus, which is a common depiction.

From Eq. (28), it is clear that the radial distribution of the GRIN medium depends on the nature of the function $q(r)$. This function's existence and explicit form depend on the origin of the ray's trajectory. Determining this function can be particularly challenging if we focus on the paths of photons around equatorial black holes. This task requires prior knowledge of the theory of relativity and tensor calculus, as well as an understanding of the nature and geometric properties of spacetime, as discussed in Sec. II.

V. RECONSTRUCTION WITHOUT GENERAL RELATIVITY

So far, in Sec. IV, we have outlined the procedure to obtain the analytical form of the GRIN medium that reproduces null geodesics around equatorial Kerr black holes. Obtaining

$q(r)$ in a broader context requires understanding general relativity, which can be challenging for a non-expert. Moreover, the analysis can take significant time, which may not be necessary if the main goal is reconstructing the GRIN medium. We will now explain how using Eq. (24) enables a remarkable simplification of the process when focusing exclusively on the trajectory.

Recent findings demonstrate that the value of K can be determined independently of the GRIN distribution, as shown below [38]:

$$K = Rn_e \sin \theta_{Inc}, \quad (33)$$

where n_e is the external refractive index in which the GRIN distribution is immersed, and θ_{Inc} is the angle of incidence of the straight light ray over the GRIN surface at the position \mathbf{r}_0 , as shown in Fig. 4.

Therefore, if the trajectory of a light ray is known, from Eqs. (23) and (33), it follows that the refractive index of the medium that reproduces such a trajectory can be calculated using the following equation:

$$n(r) = \frac{Rn_e \sin \theta_{Inc}}{r \sin \varphi(r)}. \quad (34)$$

The trajectory from which we will take inspiration to obtain the GRIN medium can come from previous research on null geodesics. These geodesics may be described using different parameterizations from those presented in this paper or may involve more complex mathematical or algorithmic methods to compute them. In earlier works, null geodesics could also result from specialized treatments of orbital families. In all these cases, we do not need to understand the detailed calculations behind these trajectories to reconstruct the GRIN medium that matches photon trajectories. We only need the ray's path. In other contexts, such as the motion of mechanical particles, trajectories may be based on experimental data.

We assume the ray is discretized to develop a systematic method for reconstructing the GRIN. Consider a discretized ray passing through a spherical GRIN lens, as illustrated in Fig. 4. Let $\mathbf{r}_i = (x_i, y_i)$ represent the points along the ray path, where i denotes the discretization index. According to Eq. (34), the value of the index of refraction at point \mathbf{r}_i along the ray's trajectory is given by

$$n(r_i) = \frac{Rn_e \sin \theta_{Inc}}{r_i \sin \varphi(r_i)}, \quad (35)$$

where $r_i = \sqrt{x_i^2 + y_i^2}$. This expression can be quickly evaluated when the trajectory is known because $\varphi(r_i)$ is calculated as [20]

$$\varphi_i = \arccos(\hat{\mathbf{r}}_i \cdot \hat{\mathbf{s}}_i), \quad (36)$$

where

$$\hat{\mathbf{r}}_i = \frac{(x_i, y_i)}{r_i}, \quad \hat{\mathbf{s}}_i = \frac{(x_{i+1} - x_i, y_{i+1} - y_i)}{\sqrt{(x_{i+1} - x_i)^2 + (y_{i+1} - y_i)^2}}. \quad (37)$$

Evaluating Eq. (35) at each point r_i enables the construction of an exact numerical method, referred to as the Physical GRIN Reconstruction (PhysGRIN) method [20]. The accuracy of the results depends on the proximity between r_i and r_{i+1} , as well as the precision of the computational tools used. The robustness of this approach allows the GRIN distribution to be reconstructed from a ray propagating around Kerr black holes. Since the physical system is not approximated, the PhysGRIN method is considered exact. This method is likely the most straightforward approach to reconstructing GRIN media in spherically symmetric cases. Furthermore, it does not require an in-depth understanding of the theory behind null geodesics; instead, implementing the algorithm is sufficient.

In Sec. VI, the PhysGRIN method is applied to reconstruct the GRIN medium representing the equatorial spacetime of a Kerr black hole. These reconstructions are then compared to the analytical solution provided by Eq. (30).

VI. RESULTS

The photon trajectories in Figs. 5–7 (a) and (d) were calculated numerically using Eq. (20) in Planck units with $m_b = 1$, employing the trapezoidal method with 10,000,000 regular divisions and choosing $x_0 = 0.001 + 0.5r_{bl,+}$. In all cases, the geodesic ends at $R = 4$. Planck units were used, and $m_b = 1$.

The index of refraction in Figs. 5–7 (b), (c), (e), and (f) was evaluated by considering the GRIN medium immersed in vacuum ($n_e = 1$). Although the analytical expressions of the index of refraction in Eq. (30) can be evaluated within the exterior of the event horizon, only the trajectories outside this region are necessary when addressing gravitational lensing effects. Thus, we avoid the interior of the black hole.

In Fig. 5, we present (a) a prograde trajectory ($h = 2.8444$) and (d) a retrograde trajectory ($h = -6.832$) for a Kerr black hole with angular momentum $a = 0.9$. Based on these trajectories, the analytical refractive index distributions are given by Eq. (30).

The refractive index distribution for the prograde trajectory is shown in Fig. 5(b), while that for the retrograde trajectory is depicted in Fig. 5(e). Figs. 5(c) and (f) compare the analytical distributions with the numerical reconstructions obtained using the PhysGRIN method for both trajectories.

To evaluate the overall accuracy of the numerical reconstruction, we use the normalized root mean square error (NRMSE), defined as:

$$\text{NRMSE} = \sqrt{\frac{\sum_{i=1}^m |n(r_i) - \hat{n}(r_i)|^2}{\sum_{i=1}^m |n(r_i)|^2}}, \quad (38)$$

where $n(r_i)$ represents the analytical distribution at point r_i , $\hat{n}(r_i)$ is the corresponding numerical reconstruction and m is the total number of discretization points ($i = 1, 2, \dots, m$). Lower NRMSE values indicate less residual variance, meaning a better approximation. Here, we choose $m = 10,000$.

The NRMSE is 9.4615×10^{-5} for the prograde trajectory. For the retrograde trajectory, the index of refraction was limited to $n < 4$ because it diverges at the position where the trajectory transitions from retrograde to prograde, causing significant numerical errors; in such conditions, the NRMSE is 2.6884×10^{-4} .

Another interesting case arises when $a = 0$ in Eq. (30) corresponds to the Schwarzschild scenario. In this case, the refractive index distribution is given by:

$$n_s(r) = n_e \sqrt{\frac{1 + 2mh^2/r^3}{1 + 2mh^2/R^3}}. \quad (39)$$

This result agrees with Ref. 14, although they do not give the explicit form of the constant coefficient.

In Fig. 6, we present the trajectories for (a) $h = 1$ and (d) $h = 5.196$. The refractive index distributions for these trajectories are shown in Fig. 6 (b) and (e), respectively. Figs. 6 (c) and (f) compare the analytical distributions with the numerical reconstructions obtained using the PhysGRIN method for both trajectories. For $h = 1$, the NRMSE is 5.3385×10^{-6} , and for $h = 5.196$, it is 2.8792×10^{-5} .

Finally, a particular case to be considered, as their analytical expression can be obtained straightforwardly, is radial geodesics ($a = h$) described by Eq. (11). These are associated

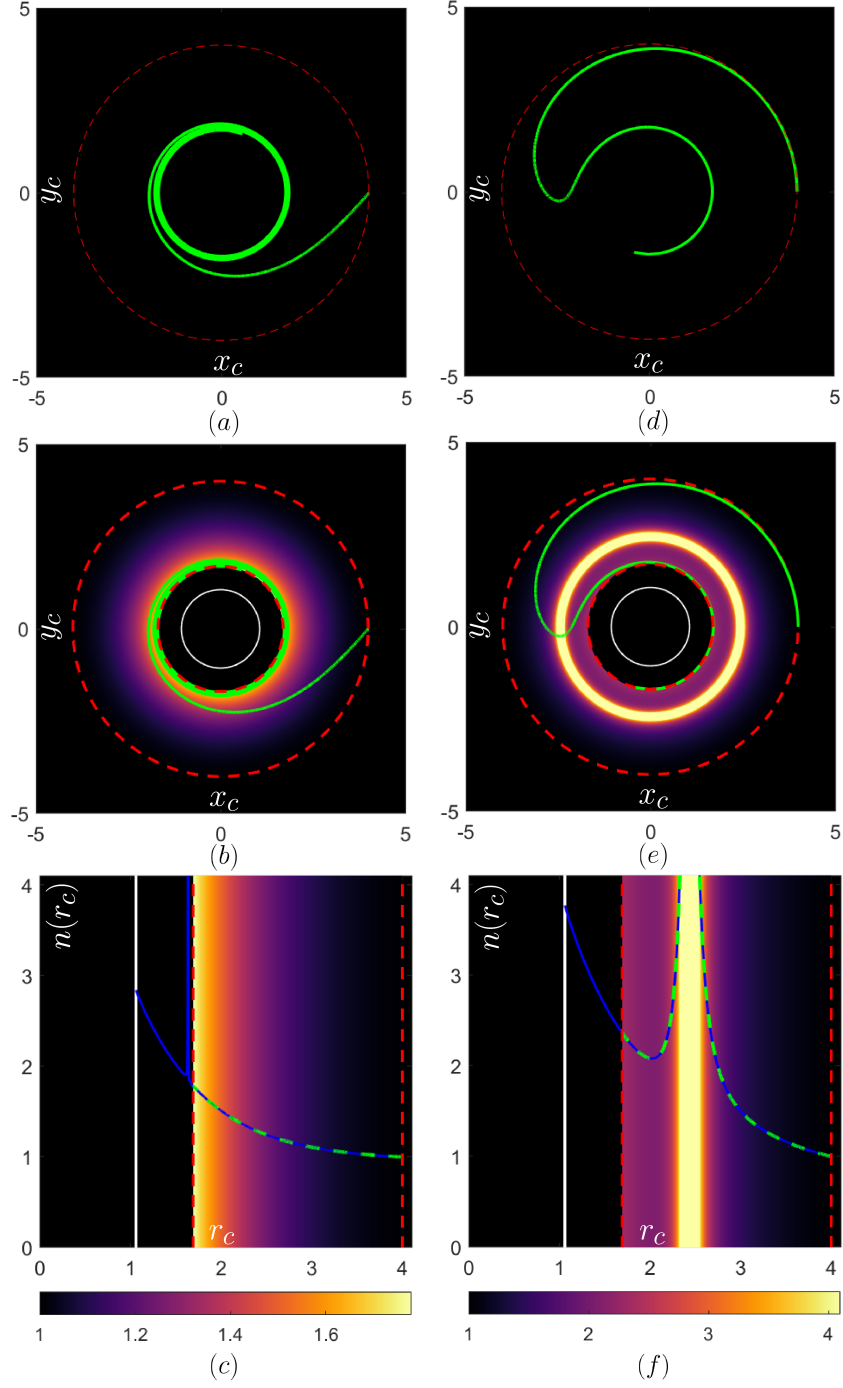


FIG. 5. **Kerr case:** Null geodesics for $a = 0.9$ with (a) $h = 2.844$ and (d) $h = -6.832$, using Planck units and $m_b = 1$. The corresponding GRIN media are shown in (b) and (e). Figures (c) and (f) compare the exact gradient index (blue line) and PhysGRIN (green dashed line). The GRIN medium is reconstructed between the outer event horizon and $R = 4$. The white line indicates the Cauchy horizon.

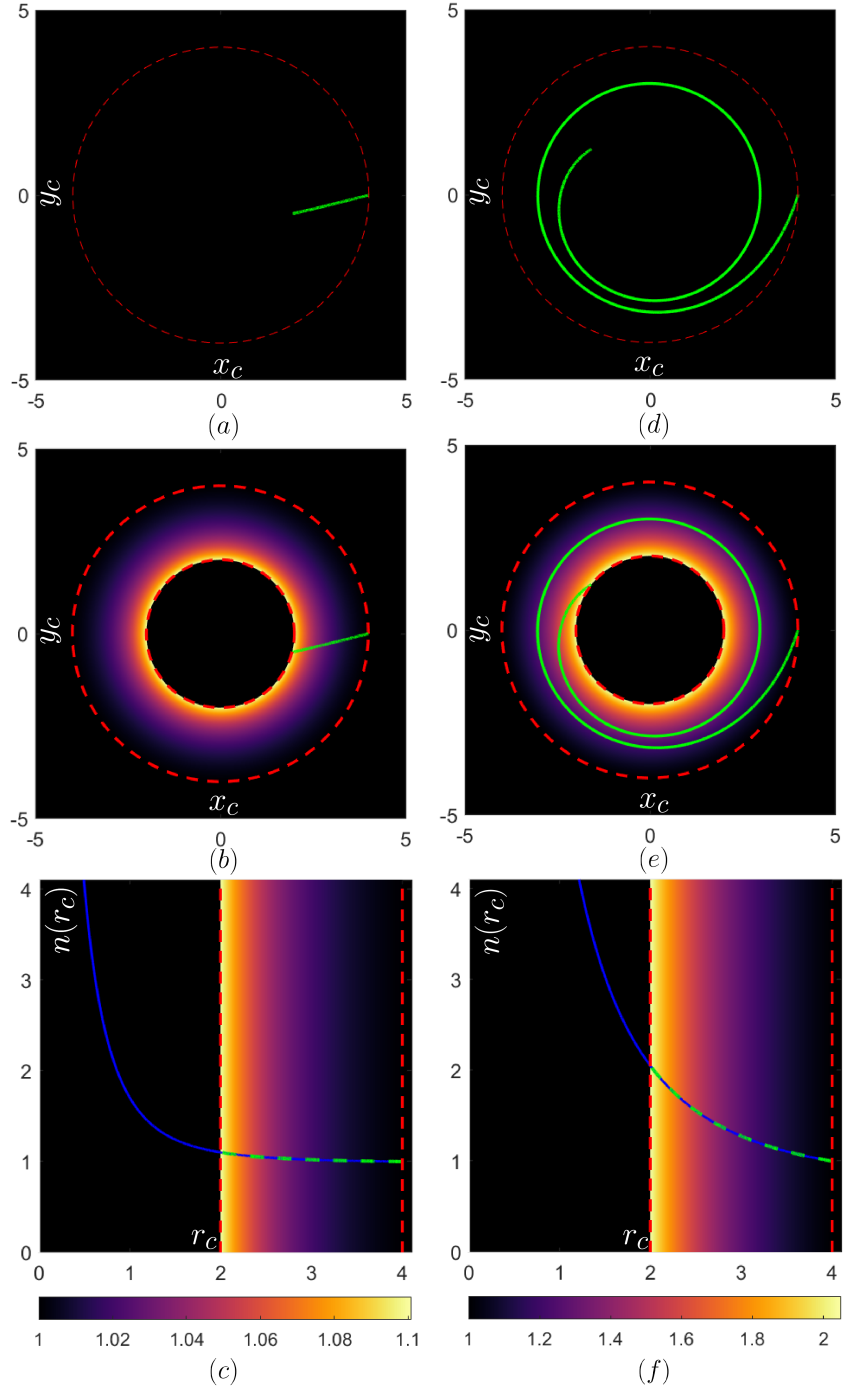


FIG. 6. **The Schwarzschild case:** Null geodesics for (a) $h = 1$ and (d) $h = 5.196$, using Planck units and $m_b = 1$. The corresponding GRIN media are shown in (b) and (e). Figures (c) and (f) compare the exact gradient index (blue line) and PhysGRIN (green dashed line). The GRIN medium is reconstructed between the Schwarzschild radius $r_c = 2$ and $R = 4$.

with the following index of refraction:

$$n_r(r) = n_e \frac{R^3}{r^3} \sqrt{\frac{r^4 a^2 + (r^2 - 2m_b \sqrt{r^2 - a^2})^2 (r^2 - a^2)}{R^4 a^2 + (R^2 - 2m_b \sqrt{R^2 - a^2})^2 (R^2 - a^2)}}. \quad (40)$$

In Fig. 7, the trajectories for (a) $a = 0.1$ and (d) $a = 0.9$ are presented. A comparison of Figs. 1 and 7 demonstrates that the numerical solution of Eq. (20) provides an adequate level of accuracy.

The refractive index distributions for these trajectories are shown in Figs. 7 (b) and (e), respectively. Figs. 7 (c) and (f) compare the analytical distributions with the numerical reconstructions obtained using the PhysGRIN method for both trajectories. For $a = 0.1$, the NRMSE is 5.3528×10^{-5} , and for $a = 0.9$ is 5.1586×10^{-5} .

Figs. 7 (c) and (f) show that, when the GRIN medium is considered to be in vacuum, the index of refraction must be less than 1, which would imply a speed of light greater than c . This issue can be addressed by immersing the GRIN in a homogeneous medium with an appropriate value of n_e . Figs. 8 (a) and (b) illustrate the cases from Fig. 7 (c) and (f) but considering $n_e = 1/0.0999$ and $n_e = 1/0.7850$, respectively, thus ensuring that the minimum value of the index of refraction is equal to 1.

All the results presented in this section confirm that GRIN media effectively reproduces the null geodesic and demonstrate the feasibility of using a simple method for reconstructing the GRIN medium without relying on complex techniques. It only requires the ray trajectory through the black hole. This highlights the simplicity of the exact numerical method, which is one of the main objectives of the present work.

VII. UNSTABLE GRIN MEDIA FOR RADIAL GEODESICS OF THE SCHWARZSCHILD BLACK HOLE

Numerically, issues are expected when computing the GRIN medium for trajectories close to the radial geodesic ($h \rightarrow 0$), as in this case $K \rightarrow 0$, which may introduce errors in the numerator of Eq. (35) under such conditions.

On the other hand, from the analytical expression in Eq. (39), when $h = 0$ and $r \neq 0$, the index of refraction remains constant and equal to n_e , which is expected for a straight light ray moving toward the origin, interestingly, in Ref. 14, although their expression for the

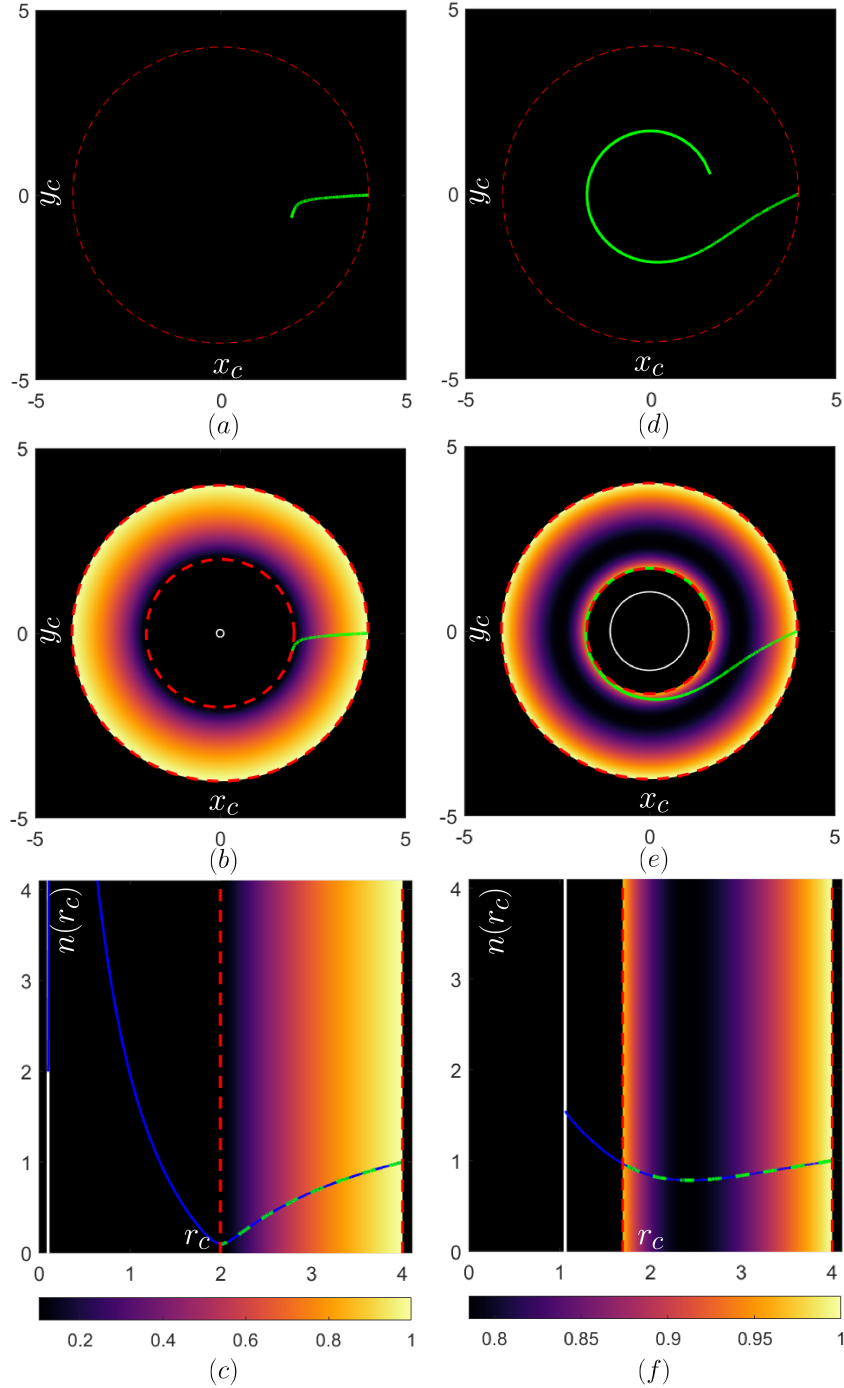


FIG. 7. **The radial geodesics ($h = a$):** Null geodesics for (a) $h = 0.1$ and (d) $h = 0.9$, using Planck units and $m_b = 1$. The corresponding GRIN media are shown in (b) and (e). Figures (c) and (f) compare the exact gradient index (blue line) and PhysGRIN (green dashed line). The GRIN medium is reconstructed between the outer event horizon and $R = 4$. The white line indicates the Cauchy horizon.

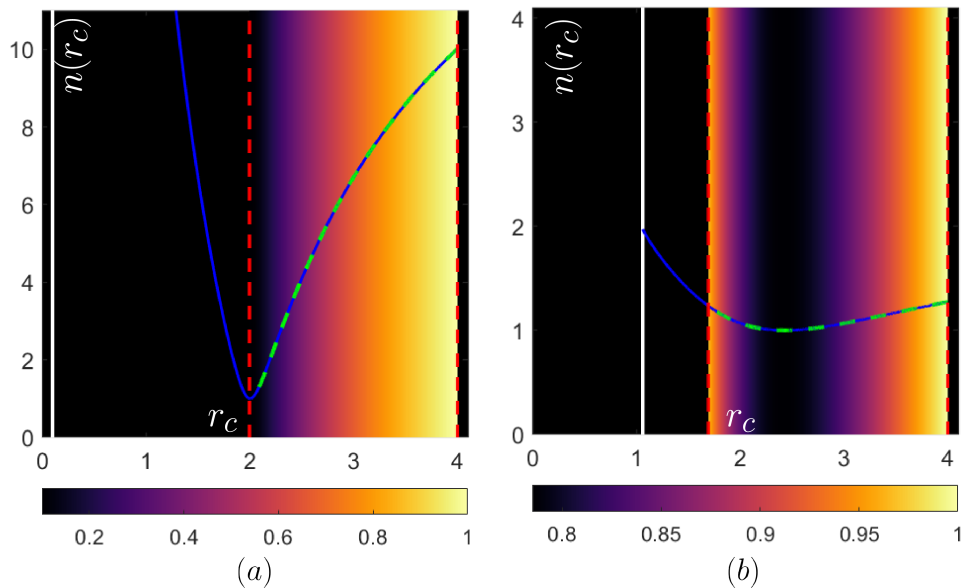


FIG. 8. The gradient index for radial geodesics ($h = a$) for the cases (a) $h = 0.1$ and $n_e = 1/0.0999$, and (b) $h = 0.9$ and $n_e = 1/0.7850$, using Planck units and $m_b = 1$. The GRIN medium is reconstructed between the outer event horizon and $R = 4$. The white line indicates the Cauchy horizon.

index of refraction is nearly identical, for the radial geodesic it tends to infinity throughout the space. This discrepancy arises because their unspecified constant of proportionality does not seem to depend on h .

On the other hand, when $h \neq 0$, Eq. (39) predicts an infinite value for the index of refraction at $r = 0$, which is consistent with the fact that light cannot traverse or escape from the black hole. Mathematically, the index of refraction for the radial geodesic ($h = 0$) at $r = 0$ is undefined. One might be tempted to define the index of refraction for the radial geodesic by asymptotically approaching $h \rightarrow 0$, which would result in a constant index of refraction throughout space, except at $r = 0$ where its value becomes infinite. This appears to be consistent with a static black hole model. However, if we approach the radial geodesic by setting $a \rightarrow 0$ in Eq. (40), we obtain:

$$n_{s,r}(r) = n_e \frac{R^2}{r^2} \left| \frac{r^2 - 2m_b r}{R^2 - 2m_b R} \right|. \quad (41)$$

This expression has a completely different behavior than that derived from Eq. (39) and yields an index of refraction of zero at the event horizon, which is not physically meaningful

in optics. Furthermore, if we set $h = 0$ in Eq. (30) and take the limit $a \rightarrow 0$, we obtain:

$$n(r) = n_e \frac{R}{r} \left| \frac{r^2 - 2m_b r}{R^2 - 2m_b R} \right|. \quad (42)$$

This results in yet another different expression for the index of refraction for the radial geodesic. In this case, the index of refraction is well-defined at $r = 0$, which is inconsistent with the black hole model, as it allows light to traverse the black hole.

These discrepancies in the index of refraction when $h = 0$ and $a = 0$ demonstrate that there is no well-defined limit for the index of refraction for a radial geodesic in the Schwarzschild black hole, indicating that the index of refraction is unstable for radial geodesics. In experiments, this instability means that null geodesics close to the radial geodesics should be avoided.

VIII. DISCUSSION AND CONCLUSIONS

In this work, we presented a methodology based on the numerical PhysGRIN method to derive GRIN media replicating photon trajectories in the curved spacetime around equatorial Kerr black holes. This approach leverages the system's symmetry and known photon trajectories, enabling the construction of GRIN media without requiring advanced knowledge of general relativity or tensor calculus. The method is founded on the conservation of Fermat's ray invariant, offering a robust and flexible numerical tool for modeling complex optical media.

We used Cartesian coordinates to represent ray trajectories because they represent the Kerr black hole singularity as an annulus, a widely accepted depiction.

Additionally, by applying the conservation of Fermat's ray invariant, we derived an analytical form of the GRIN medium for equatorial null geodesics around Kerr black holes in Cartesian coordinates. In contrast, Ref. 14 provided expressions in Boyer-Lindquist coordinates, differing from ours except in the Schwarzschild case, where they coincide up to a constant, leading to additional issues for radial geodesics.

Our results align with the suggestion of Ref. 18 that the most accurate definition of the index of refraction compares null geodesics in spacetime to light rays in optical media. This approach is particularly effective when focusing solely on ray trajectories without considering additional electromagnetic wave properties such as polarization.

Overall, the PhysGRIN method provides a framework for deriving GRIN media from known light paths, producing an index of refraction that matches the system’s geodesics. While the results depend on how light rays are represented in a specific coordinate system, this approach remains independent of alternative conceptual interpretations of the index of refraction, as evidenced by the various definitions proposed for the Schwarzschild case [18]. By relying solely on the symmetries of light paths, the method can also be extended to mimic particle trajectories in classical and quantum mechanics (including Bohmian trajectories) [40, 41]. This makes GRIN media a valuable tool for visualizing phenomena across various scales, from quantum systems to macroscopic scenarios.

Disclosures

The authors declare that there are no financial interests, commercial affiliations, or other potential conflicts of interest that could have influenced the objectivity of this research or the writing of this paper.

Code Availability

Data may be obtained from the authors upon reasonable request.

Acknowledgments

The authors acknowledge the support of the Instituto Nacional de Astrofísica, Óptica y Electrónica (INAOE), the Consejo Nacional de Humanidades, Ciencias y Tecnologías (CONAHCYT), and the Sistema Nacional de Investigadoras e Investigadores (SNII) for this publication.

[1] M. Grespan and M. Biesiada, “Strong gravitational lensing of gravitational waves: A review,” *Universe* **9**, 200 (2023). [doi:10.3390/universe9050200].

- [2] V. Rodríguez-Fajardo, T. P. Nguyen, K. S. Hocek, *et al.*, “Einstein beams and the diffractive aspect of gravitationally-lensed light,” *New J. Phys.* **25**, 083033 (2023). [doi:10.1088/1367-2630/ace98e].
- [3] V. Perlick, “Gravitational lensing from a spacetime perspective,” *Living Rev. Rel.* **7** (2004). [doi:10.12942/lrr-2004-9].
- [4] M. Bartelmann, “Gravitational lensing,” *Class. Quantum Grav.* **27**, 233001 (2010). [doi:10.1088/0264-9381/27/23/233001].
- [5] F. J. Raab and D. H. Reitze, “The first direct detection of gravitational waves opens a vast new frontier in astronomy,” *Curr. Sci* **113**, 657 (2017). [doi:10.18520/cs/v113/i04/657-662].
- [6] D. Castelvecchi, “Black hole pictured for first time — in spectacular detail,” *Nature* **568**, 284–285 (2019). [doi:10.1038/d41586-019-01155-0].
- [7] J. Plebanski, “Electromagnetic waves in gravitational fields,” *Phys. Rev.* **118**, 1396–1408 (1960). [doi:10.1103/physrev.118.1396].
- [8] F. de Felice, “On the gravitational field acting as an optical medium,” *Gen. Relativ. Gravit.* **2**, 347–357 (1971). [doi:10.1007/bf00758153].
- [9] R. Schützhold and W. G. Unruh, “Gravity wave analogues of black holes,” *Phys. Rev. D* **66** (2002). [doi:10.1103/physrevd.66.044019].
- [10] T. G. Philbin, C. Kuklewicz, S. Robertson, *et al.*, “Fiber-optical analog of the event horizon,” *Science* **319**, 1367–1370 (2008). [doi:10.1126/science.1153625].
- [11] D. A. Genov, S. Zhang, and X. Zhang, “Mimicking celestial mechanics in metamaterials,” *Nat. Phys.* **5**, 687–692 (2009). [doi:10.1038/nphys1338].
- [12] H. Chen, R.-X. Miao, and M. Li, “Transformation optics that mimics the system outside a Schwarzschild black hole,” *Opt. Express* **18**, 15183 (2010). [doi:10.1364/oe.18.015183].
- [13] U. Leonhardt and T. Philbin, *Geometry and light: the science of invisibility*, Courier Corporation, Mineola, New York (2010).
- [14] R. A. Tinguely and A. P. Turner, “Optical analogues to the equatorial Kerr–Newman black hole,” *Commun. Phys.* **3** (2020). [doi:10.1038/s42005-020-0384-5].
- [15] P. Švančara, P. Smaniotto, L. Solidoro, *et al.*, “Rotating curved spacetime signatures from a giant quantum vortex,” *Nature* **628**, 66–70 (2024). [doi:10.1038/s41586-024-07176-8].
- [16] W. Gordon, “Zur lichtfortpflanzung nach der relativitätstheorie,” *Ann. Phys.* **377**, 421–456 (1923). [doi:10.1002/andp.19233772202].

- [17] I. Kovner, “Fermat principle in arbitrary gravitational fields,” *Astrophys. J.* **351**, 114 (1990). [doi:10.1086/168450].
- [18] H. Ramezani-Aval, “A comparative study on the gravitational analog of the spacetime index of refraction,” *Chin. J. Phys.* **88**, 69–76 (2024). [doi:10.1016/j.cjph.2024.01.016].
- [19] I. A. Kogan and P. J. Olver, “Invariant Euler–Lagrange equations and the invariant variational bicomplex,” *Acta Appl. Math.* **76**, 137–193 (2003). [doi:10.1023/A:1022993616247].
- [20] J. E. Gómez-Correa, A. L. Padilla-Ortiz, J. P. Trevino, *et al.*, “Symmetric gradient-index media reconstruction,” *Opt. Express* **31**, 29196 (2023). [doi:10.1364/oe.498649].
- [21] P. Schneider, J. Ehlers, and E. E. Falco, *Gravitational Lenses*, Springer Berlin Heidelberg (1992). [doi:10.1007/978-3-662-03758-4].
- [22] R. H. Price and K. S. Thorne, “Lagrangian vs Hamiltonian: The best approach to relativistic orbits,” *Am. J. Phys.* **86**, 678–682 (2018). [doi:10.1119/1.5047439].
- [23] K. S. Thorne, C. W. Misner, and J. A. Wheeler, *Gravitation*, W. H. Freeman and Company, San Francisco (2000).
- [24] L. D. Landau and E. M. Lifshitz, *Mechanics*, vol. 1, CUP Archive (1960).
- [25] J. Wambsganss, “Gravitational lensing in astronomy,” *Living Rev. Rel.* **1**, 1–74 (1998). [doi:10.12942/lrr-1998-12].
- [26] J. M. McNamara, “Instability of black hole inner horizons,” *Proc. Roy. Soc. Lon. A* **358**(1695), 499–517 (1978). [doi:10.1098/rspa.1978.0024].
- [27] J. Dexter and E. Agol, “A fast new public code for computing photon orbits in a Kerr spacetime,” *Astrophys. J.* **696**, 1616–1629 (2009). [doi:10.1088/0004-637x/696/2/1616].
- [28] X. Yang and J. Wang, “Ynogk: A new public code for calculating null geodesics in the Kerr spacetime,” *Astrophys. J. Suppl.* **207**, 6 (2013). [doi:10.1088/0067-0049/207/1/6].
- [29] Z. Fan and H. Feng, “The exact solution to null geodesics at the equatorial plane in kerr spacetime,” *College Physics* **37** (2018). [doi:10.16854/j.cnki.1000-0712.170603].
- [30] S. E. Gralla and A. Lupsasca, “Null geodesics of the Kerr exterior,” *Phys. Rev. D* **101** (2020). [doi:10.1103/physrevd.101.044032].
- [31] A. Cieřlik, E. Hackmann, and P. Mach, “Kerr geodesics in terms of Weierstrass elliptic functions,” *Phys. Rev. D* **108** (2023). [doi:10.1103/physrevd.108.024056].
- [32] Y. Liu and B. Sun, “Analytical solutions of equatorial geodesic motion in Kerr spacetime*,” *Chinese Phys. C* **48**, 045107 (2024). [doi:10.1088/1674-1137/ad260a].

- [33] S. Chandrasekhar, *The Mathematical Theory of Black Holes*, Oxford University Press Oxford (1998). [doi:10.1093/oso/9780198503705.001.0001].
- [34] I. S. Gradshteyn and I. M. Ryzhik, *Table of Integrals, Series, and Products*, Academic Press, Singapore, 6th ed. (2000).
- [35] N. Bretón, O. d. J. Cabrera-Rosas, E. Espíndola-Ramos, *et al.*, “Towards the Ronchi test for gravitational lenses: the gravitoronchigram,” *J. Opt.* **19**, 065602 (2017). [doi:10.1088/2040-8986/aa6cc7].
- [36] V. Lakshminarayanan, A. K. Ghatak, and K. Thyagarajan, *Lagrangian optics*, Springer (2002).
- [37] J. E. Gómez-Correa, A. L. Padilla-Ortiz, A. Jaimes-Nájera, *et al.*, “Generalization of ray tracing in symmetric gradient-index media by Fermat’s ray invariants,” *Opt. Express* **29**, 33009–33026 (2021). [doi:10.1364/OE.440410].
- [38] J. E. Gómez-Correa, “Geometrical-light-propagation in non-normalized symmetric gradient-index media,” *Opt. Express* **30**, 33896–33910 (2022). [doi:10.1364/OE.465957].
- [39] M. Born and E. Wolf, *Principles of Optics: 60th Anniversary Edition*, Cambridge University Press (2019). [doi:10.1017/9781108769914].
- [40] W. Xiao, S. Tao, and H. Chen, “Mimicking the gravitational effect with gradient index lenses in geometrical optics,” *Photonics Res.* **9**, 1197 (2021). [doi:10.1364/prj.418787].
- [41] O. de Alcantara Bonfim, J. Florencio, and F. Sá Barreto, “Chaotic Bohm’s trajectories in a quantum circular billiard,” *Phys.Lett.A* **277**, 129–134 (2000). [doi:10.1016/s0375-9601(00)00705-2].